Deep Learning for Causal Inference

A Comparison of Architectures for Heterogeneous Treatment Effect Estimation

> Demetrios Papakostas Andrew Herren P. Richard Hahn Francisco Castillo

Abstract

Causal inference has gained much popularity in recent years, with interests ranging from academic, to industrial, to educational, and all in between. Concurrently, the study and usage of neural networks has also grown profoundly (albeit at a far faster rate). What we aim to do in this blog write-up is demonstrate a Neural Network causal inference architecture. We develop a fully connected neural network implementation of the popular Bayesian Causal Forest algorithm, a state of the art tree based method for estimating heterogeneous treatment effects. We compare our implementation to existing neural network causal inference methodologies, showing improvements in performance in simulation settings. We apply our method to a dataset examining the effect of stress on sleep.

1 Introduction

A common problem in causal inference is to infer the effect of a binary treatment, Z, on a scalar-valued outcome Y. When the effect of Z on Y is posited to be constant for all subjects, or homogeneous, the estimand of interest (average treatment effect) is a scalar-valued parameter, which admits a number of common estimators. When the assumption of treatment effect homogeneity is unwarranted, estimates of the average treatment effect (ATE) may be of questionable utility. The challenge of estimating a heterogeneous conditional average treatment effect (CATE), is evident in the fact that the estimand is no longer a scalar-valued parameter but a function of a (potentially high dimensional) covariate vector X. In recent years, researchers have proposed to use machine learning methods for nonparametric CATE estimation (Hahn et al. [2020]; Krantsevich et al. [2021], Hill [2011]; Wager and Athey [2018]; Farrell et al. [2020]). Additional methods that have been introduced include TARNET (Shalit et al. [2017]), Dragonnet (Shi et al. [2019]) and that of Chen and Liu [2018]. The main focus of this document will be comparing Farrell et al. [2020] and the method we introduce, as they are the most similar in nature.

This paper focuses specifically on CATE estimators that rely on deep neural networks. While neural networks are universal function approximators (Cybenko [1989]), nature does not typically provide treatment effects for use as "training data," and estimation proceeds by defining networks that can infer the CATE from available data. The architecture of a deep neural network, which refers to a specific composition of weights, data, and activation functions, plays a crucial role in this process, along with regularization and training techniques. This paper compares empirical CATE estimates of several architectures. The first two methods represent outcomes as a sum of the CATE, $\beta(X)$, and the prognostic effect $\alpha(X)$, which occurs regardless of treatment status. In the Farrell et al. [2020] architecture, both $\alpha(X)$ and $\beta(X)$ emerge from a shared set of hidden layers. Essentially, this architecture learns a common set of basis functions for $\alpha(X)$ and $\beta(X)$ and then estimates separate coefficients for each those basis functions. We refer to this approach as "the Farrell method" or simply "Farrell" for the remainder of the paper. The second method an extension of Bayesian Causal Forests (BCF) (Hahn et al. [2020]). This method, which we hereafter refer to as "BCF-nnet" or "nnet BCF," uses completely separate neural networks for $\alpha(X)$ and $\beta(X)$. Finally, we consider a "naive" approach that partitions the data into treatment and control groups, and learns a separate function on each subset of the data. These functions can be used to estimate the CATE by subtracting predictions of the "treatment function" from those of the "control function."

Simulation studies show that nnet BCF outperforms both the Farrell and naive methods when treatment effects are small relative to prognostic effects.

2 Problem Description

In order to make the problem precise, we begin by introducing notation and defining our estimators. We will use the following conventions in our notation:

- Bold upper case letters (i.e. X) refer to random matrices
- Bold lower case letters (i.e. x) refer to instantiations of random matrices
- lacktriangle Regular upper case letters (X, Y, Z) refer to random variables / vector
- Regular lower case letters (x, y, z) refer to instantiations of random variables
- Math calligraphy letters $(\mathcal{X}, \mathcal{Y}, \mathcal{Z})$ refer to the support of a random variable

For example, if $X \sim f(X)$, we could write $\mathbb{E}(X) = \int_{\mathscr{X}} x f(x) dx$.

Causal inference is concerned with the effect of a treatment, which we denote as Z, on an outcome Y. In general, both the treatment and outcome can be continuous, categorical, or binary. For the purposes of this paper, we restrict our attention to the case of a binary treatment ($\mathcal{Z} = \{0,1\}$) and a continuous outcome ($\mathscr{Y} = \mathbb{R}$).

Our overview of the causal inference assumptions largely follows that of Hernán and Robins [2020]. We are interested in inferring the effect of a treatment, or intervention, on an outcome when nothing is changed except the treatment being administered. In experimental settings, this

causal interpretation is often provided by the study design (randomized controlled trial, randomized block design, etc...). In many real-world scenarios, designing and conducting an experiment would be impossible, unethical, or highly impractical. In such cases, investigators are limited to using observational data (i.e. data that were not collected from a designed experiment).

To formalize the idea described above, we let Y^1 and Y^0 denote two counterfactual random variables, where Y^i indexes the random outcomes for cases in which Z has been set equal to i. The counterfactual nature of these random variables is important to underscore before we define assumptions and estimators. These two random variables are often referred to as *potential outcomes* (see for example Hernán and Robins [2020]). The variables are random because even in the counterfactual scenario in which only treatment i has been administered, Y may potentially be influenced by other factors.

We can define the average treatment effect (ATE) as $\beta = \mathbb{E}\left(Y^1 - Y^0\right) = \mathbb{E}\left(Y^1\right) - \mathbb{E}\left(Y^0\right)$. In many classical statistical problems, inferring the difference of two random variables is as straightforward as assessing the difference in the empirical means of samples of both random variables. However, the counterfactual nature of Y^1 and Y^0 is such that for any observation, only one of the two variables can be observed (subjects cannot receive both the treatment and control). We define the observable random variable $Y = ZY^1 + (1-Z)Y^0$. In order to use a dataset of independent and identically distributed (iid) samples of Z and Y to estimate the ATE, we must make several identifying assumptions.

- 1. Exchangeability: $Y^1, Y^0 \perp Z$
- 2. *Positivity*: 0 < P(Z = 1) < 1
- 3. Stable Unit Treatment Value Assumption (SUTVA): $Y_i^1, Y_i^0 \perp Y_j^1, Y_j^0$ for all $j \neq i$

With these assumptions, we can use observed data to estimate the average treatment effect. One common estimator is the "inverse propensity weighted" (IPW) estimator, whose expectation is shown

below to be the ATE under the three assumptions of exchangeability, positivity, and SUTVA.

$$\begin{split} \frac{YZ}{p(Z=1)} - \frac{Y(1-Z)}{1-p(Z=1)} &= \frac{\left(Y^1Z + Y^0(1-Z)\right)Z}{p(Z=1)} - \frac{\left(Y^1Z + Y^0(1-Z)\right)(1-Z)}{1-p(Z=1)} \\ &= \frac{Y^1Z^2 + Y^0(1-Z)Z}{p(Z=1)} - \frac{Y^1Z(1-Z) + Y^0(1-Z)^2}{1-p(Z=1)} \\ &= \frac{Y^1Z}{p(Z=1)} - \frac{Y^0(1-Z)}{1-p(Z=1)} \\ &\mathbb{E}\left(\frac{YZ}{p(Z=1)} - \frac{Y(1-Z)}{1-p(Z=1)}\right) = \mathbb{E}\left(\frac{YZ}{p(Z=1)}\right) - \mathbb{E}\left(\frac{Y(1-Z)}{1-p(Z=1)}\right) \\ &= \mathbb{E}\left(\frac{Y^1Z}{p(Z=1)}\right) - \mathbb{E}\left(\frac{Y^0(1-Z)}{1-p(Z=1)}\right) \\ &= \mathbb{E}\left(Y^1\right)\mathbb{E}\left(\frac{Z}{p(Z=1)}\right) - \mathbb{E}\left(Y^0\right)\mathbb{E}\left(\frac{1-Z}{1-p(Z=1)}\right) \\ &= \mathbb{E}\left(Y^1\right)\frac{p(Z=1)}{p(Z=1)} - \mathbb{E}\left(Y^0\right)\frac{1-p(Z=1)}{1-p(Z=1)} \\ &= \mathbb{E}\left(Y^1\right) - \mathbb{E}\left(Y^0\right) \end{split}$$

In practice, P(Z = 1) is often estimated from the data, but as long as $\mathbb{E}(\hat{p}(Z = 1)) = p(Z = 1)$, the estimator will still be unbiased.

IPW is just one of many estimators of the average treatment effect. We refer the interested reader to Hernán and Robins [2020] for more detail. We now introduce the random variable X to denote a vector of *covariates* of the outcome (often referred to as "features" in machine learning). These covariates might include demographic variables, health markers measured before treatment administration, survey variables measuring attitudes or preferences, and so on.

Consider a simple motivating example, in which X is age, Z is a blood pressure medication, and Y is blood pressure. Older patients are more likely to have high blood pressure, so we would expect that X and Y are not independent. Older patients, who visit the doctor more frequently, are also potentially more likely to be prescribed blood pressure medicine. In this case, we would not expect $Y^1, Y^0 \perp Z$. Older patients are more likely to receive blood pressure medicine and also more likely to have high blood pressure so that observing Z = 1 changes the distribution of Y^1 and Y^0 .

We can work around this limitation with a modified assumption, *conditional exchangeability*: $Y^1, Y^0 \perp Z \mid X$. In words, this states that, after we control for the effect of X on treatment assignment, the data satisfy exchangeability. Similarly, we no longer have that P(Z=1) is the same for all subjects, so we modify the positivity assumption to hold that $0 < P(Z=1 \mid X) < 1$. Under this set of assumptions, we define a new IPW estimator as $\frac{YZ}{p(Z=1\mid X)} - \frac{Y(1-Z)}{1-p(Z=1\mid X)}$ and can show that its expected value is the ATE.

2.1 Conditional Average Treatment Effect (CATE)

With the notation in place, we proceed to the focus of this paper: estimating heterogeneous treatment effects using deep learning. In the prior section, we introduced the average treatment effect as an expected difference in potential outcomes across the entire support set of covariates. Average treatment effects have a long history in the causal inference literature because they are (relatively) straightforward to estimate and provide useful, intuitive information about the average benefits (or harms) of an intervention.

Sometimes, however, the ATE masks a considerable degree of heterogeneity in the causal effects of an intervention. Consider the everyday example of caffeine tolerance. Some people find that any level of caffeine consumption at any time of day carries too many unpleasant effects, while others drink espresso after a large dinner. While it may be possible to measure an average treatment effect of a given dose of caffeine, the estimate collapses a range of individual treatment effects and may thus not provide much clinical or practical insight.

We define the *Conditional Average Treatment Effect* (CATE) as $\mathbb{E}\left(Y^1-Y^0\mid X=x\right)$. Intuitively, this defines a treatment effect for the conditional distribution of Y^1 and Y^0 in which X=x. Note that with this modification we define not a single parameter β but a function $X\longrightarrow \beta(X)$. If X is binary or categorical, this can be done empirically by partitioning the data into subsets $\{x:x=s\}$ and then estimating the ATE on the subsets. But in general, with continuous X or simply a large number of categorical X variables, this approach becomes impossible and $\beta(X)$ must be estimated by fitting a model.

A tempting and convenient first step in CATE estimation would be use a linear model for $\beta(X)$. More recently, advances in computer speed and a growing recognition of the complexity of many causal processes has spurred interest in nonparametric estimators of $\beta(X)$. To name a few examples, Hahn et al. [2020] and Hill [2011] use Bayesian tree ensembles, Wager and Athey [2018] use random forests, and Farrell et al. [2020] use deep learning. The focus of this paper will be to compare the method introduced in Farrell et al. [2020] to a novel architecture inspired by Hahn et al. [2020] and a naive partition-based architecture.

2.2 Estimating CATE using Deep Learning

We adapt the notation of Farrell et al. [2020] slightly to fit the conventions used above. As in prior sections, our goal here is to estimate a causal effect of a binary treatment Z, on a continuous outcome Y. Since we are interested in the effect's heterogeneity, we must construct a model that will estimate $\mathbb{E}\left(Y^1-Y^0|X=x\right)$ for any x. Before discussing the specific architecture, we introduce some more clarifying terminology and notation. This construction of treatment effect heterogeneity follows that of Hahn et al. [2020]. Consider the following model

$$Y = \alpha(X) + \beta(X)Z + \varepsilon$$
$$\varepsilon \sim \mathcal{N}(0, \sigma_{\varepsilon})$$
$$Z \sim \text{Bernoulli}(\pi(X))$$

In this case, $\beta(X)$ corresponds to the treatment effect function, which given the assumptions in the prior section, can be written as $\mathbb{E}(Y \mid X, Z = 1) - \mathbb{E}(Y \mid X, Z = 0)$. $\alpha(X)$ corresponds to $\mathbb{E}(Y \mid X, Z = 0)$ which we refer to as the *prognostic function*, ε is random noise, and $\pi(X) = \mathbb{P}(Z = 1 \mid X)$ which we refer to as the *propensity function*.

Right now, X refers to a (potentially large) vector of covariates that may be useful in estimating heterogeneous treatment effects. But using the above notation, we can partition X into several categories:

- 1. **Prognostic** features impact Y through $\alpha(X)$
- 2. **Effect-modifying** features impact the outcome Y through $\beta(X)$
- 3. **Propensity** features impact the outcome *Y* through $\pi(X)$

For example if $\pi(X) = \sin(X_1) + |X_3|$, we would say that X_1 and X_3 are propensity variables but X_2 , for example, is not. These categories are of course not mutually exclusive, but can be made so by considering their combinations. We avoid the complete factorial expansion of these three categories and instead define several combinations that are of particular interest in methodological problems.

- 1. **Pure prognostic** variables are variables which only appear in the function $\alpha(X)$
- 2. **Pure modifiers** are variables which only appear in the function $\beta(X)$
- 3. **Pure propensity** variables are variables which only appear in the function $\pi(X)$
- 4. **Confounders** are variables which appear in both $\pi(X)$ and $\alpha(X)$

Before we proceed, we also introduce the concept of **targeted selection**, when $\pi(X) = f(\alpha(X))$. Intuitively, this corresponds to a practice of assigning treatment to those who are most likely to need it (because, for example, $\alpha(X) = \mathbb{E}(Y|X,Z=0)$ would be high otherwise). This is an extreme version of confounding, in which the entire prognostic function is an input to the propensity function and thus to the assignment of treatment. As is discussed in depth in Hahn et al. [2020], this phenomenon is both highly plausible in real-world settings and also vexing to many approaches to CATE estimation.

The architecture of the model is discussed in depth in later sections, so here we simply note the high-level differences between the Farrell method and nnet-BCF. Farrell et al. [2020] propose to fit a model $\mathbb{E}(Y) = \alpha(X) + \beta(X)Z$ using a neural network with two hidden layers to which map to two separate output nodes: $\alpha(X)$ and $\beta(X)$. Hahn et al. [2020] fit a similar model using Bayesian Additive Regression Trees (BART) (Chipman et al. [2010]), with one key distinction. $\alpha(X)$ and $\beta(X)Z$ are fit as completely separate models with no information shared during training. This is different from the Farrell et al. [2020] approach as their method shares weights between the $\alpha(X)$ and $\beta(X)$ functions via the first two hidden layers. BCF nnet follows the approach of Hahn et al. [2020] by training two completely separate neural networks for $\alpha(X)$ and $\beta(X)$. Finally, the "naive" method estimates $\mathbb{E}(Y \mid X, Z = 1)$ with one network and $\mathbb{E}(Y \mid X, Z = 0)$ with another network so that $\beta(X)$ can be estimated as a difference between these networks' predictions.

3 Methods

In this section, we discuss in more detail how the CATE is estimated in each of the three deep learning methods proposed, as well as a linear model comparison.

3.1 Joint Training Architecture (Farrell/Shared Network)

In Farrell et al. [2020], the authors posit that

$$\mathbb{E}\left(Y\mid X=x,Z=z\right)=G\left(\alpha(x)+\beta(x)z\right) \tag{1}$$

where $G(u), u \in \mathbb{R}$ is a known link function specified by the researcher, and $\alpha(\cdot)$ and $\beta(\cdot)$ are unknown functions to be estimated. Since we are interested in effects of Z on a real-valued Y, we use an identity link function so that $G(\cdot)$ can be removed from the equations and we have $\mathbb{E}(Y \mid X = x, Z = z) = \alpha(x) + \beta(x)z$. The authors propose estimating $\alpha(\cdot)$ and $\beta(\cdot)$ with one deep fully connected neural network. We implement this architecture as a fully connected neural network with two hidden layers and a two-node parameter layer which outputs $\alpha(X)$ and $\beta(X)$. The output of this architecture is then a linear combination of the two nodes in the parameters layer, $\alpha(x) + \beta(x)z$ (see Figure 1).

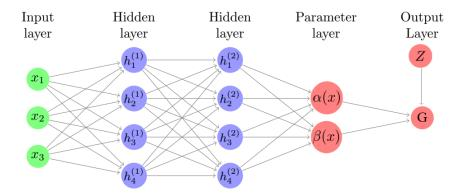


Figure 1: The Farrell method with a 3-dimensional vector of covariates X, 4 nodes in each hidden layer (in practice, these layers are usually much deeper). G is an activation function that takes $\alpha(X) + \beta(X)Z$ as an argument.

Since *Y* is real-valued, we use mean squared error (MSE) as a loss function in training each of the methods introduced in this section.

3.2 BCF nnet

Based on the results and discussion in Hahn et al. [2020], we hypothesize that splitting $\alpha(\cdot)$ and $\beta(\cdot)$ into separate networks with no shared weights may yield better CATE estimates on some data generating processes (DGPs). The BCF nnet method specifies

$$\mathbb{E}\left(Y\mid X=x,Z=z\right)=\alpha\left(x,\hat{\pi}(x)\right)+\beta(x)z\tag{2}$$

In Hahn et al. [2020], α and β are given independent BART priors (Chipman et al. [2010]). $\hat{\pi}(x_i)$ is an estimate of the propensity function We implement the BCF nnet architecture as in Figure 2. While

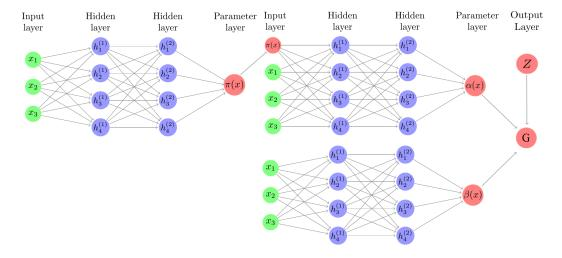


Figure 2: The BCF nnet architecture, where $G(\cdot)$ is an activation function that takes $\alpha(X) + \beta(X)Z$ as an argument.

the shared-weights versus separate weights distinction between Farrell and BCF nnet has been made clear, a subtle difference between the architectures is that BCF nnet allows for an estimate of the propensity function to be incorporated as a feature in the $\alpha(X)$ network. Since targeted selection implies $\alpha(X)$ is a function of $\pi(X)$, this parameterization was observed to be helpful in Hahn et al. [2020].

In Farrell et al. [2020], the authors develop confidence intervals for their architecture's estimates (relying on influence functions, a common tool for calculating standard errors in non-parametrics). We incorporated these intervals into our architecture, but found that they were far too tight and exhibited poor coverage in the low n settings we were studying. We therefore do not report or comment further.

3.3 Separate Network Regression Approach

The "naive" method in our comparison employs two completely separate regression models,

$$Y_1(X) = \mathbb{E}\left(Y \mid Z = 1, X\right) \text{ and } Y_0(X) = \mathbb{E}\left(Y \mid Z = 0, X\right)$$
(3)

With these two regression functions, our estimate of $\beta(X)$ is simply $\beta(X) = Y_1(X) - Y_0(X)$. Each $Y_i(X)$ is constructed as a 2-layer fully connected neural network, with the number of parameters chosen to be similar to the number chosen for the Farrell and the BCF architecture.

3.4 Linear Model

We also compare our two neural network architectures to a simple linear model's estimate of β

$$Y = \beta Z + X\delta + \varepsilon \tag{4}$$

where β is the coefficient of interest and represents the average treatment effect. The model is fit using ordinary least squares (OLS). We allow for interaction effects between X and Z.

4 Simulation Summary

Equation 5 is the first DGP we run. We choose a complex function for α and strong targeted selection, and a simpler function for β (which allows for heterogeneous effects) to illustrate the effect of targeted selection.

$$X_{1}, X_{2}, X_{3} \sim N(0, 1)$$

$$X_{4} \sim \operatorname{binomial}(n = 2, p = 0.5)$$

$$X_{5} \sim \operatorname{Bern}(p = 0.5)$$

$$X = (X_{1}, X_{2}, X_{3}, X_{4}, X_{5})$$

$$\beta(X) = \begin{cases} 0.20 + 0.5 * X_{1} \cdot X_{4} & \text{small treatment to prognosis} \\ 5 + 0.5 * X_{1} \cdot X_{4} & \text{large treatment to prognosis} \end{cases}$$

$$\alpha(X) = 0.5 \cos(2X_{1}) + 0.95 * |X_{3} \cdot X_{5}| - 0.2 * X_{2} + 1.5$$

$$\pi(X) = 0.70 * \Phi\left(\frac{\alpha(X)}{s(\alpha(X))} - 3.5\right) + u/10 + 0.10$$

$$u \sim \operatorname{uniform}(0, 1)$$

$$Y = \alpha(X) + \beta(X)Z + \sigma\varepsilon$$

$$\varepsilon \sim N(0, 1)$$

$$\sigma = \operatorname{sd}(\alpha(X)) \cdot \kappa$$

$$Z \sim \operatorname{Bern}(p = \pi(X))$$

We choose the total number of parameters in the Shared architecture to be about the same as the separate network ($\alpha + \beta$ networks). In the Shared network, this means we have 100 hidden nodes in layer 1, and 26 in layer 2, meaning 3,280 total parameters.

In the BCF NNet architecture, we have 60 parameters in the α first layer, 32 hidden nodes in the second layer. For the β network, we have 30 and 20 hidden nodes respectively. This yields 3,226 total parameters. For both methods, we use a learning rate of 0.001 with an Adam Optimizer, we use Sigmoid activation, binary cross entropy loss for the propensity, MSE for the other networks, ReLu activation (double check), 250 epochs, and a batch size of 64. The dropout rate is 0.25 in every layer. The propensity score for the BCF NNet architecture is estimated using a 2 layer fully connected neural network with 100 and 25 hidden nodes respectively, and the rest of the parameters the same as above. In the separate network approach, we build the architecture separately using a 2-layer

fully constructed neural network (for both Y_1 and Y_0 , as described in Equation 3) infrastructure with 50 hidden nodes in layer 1 and 26 in layer 2 for both models. This is a total of 3,306 parameters. The other hyperparameters are the same as the BCF NNet and Shared Network approach.

Table 1 shows results using both the Shared Network approach Farrell et al. [2020] and the BCF Nnet approach we present. This table indicates some RIC which biases the Farrell approach. The method we propose also has additional flexibility in that the propensity estimate can be estimated with any method and passed in, it need not be a MLP approach. Additionally, because we separate the networks, like in the original BCF paper Hahn et al. [2020], we can add additional regularization on the β network¹.

Table 2 shows results with a large treatment to prognosis ratio. In this setting, even with RIC presumably still being relevant due to the strong targeted selection in Equation 5 (see right panel of Figure 3), the large treatment effect dominating allows for the extra parameters of the shared network approach to out-perform the separate network approach. However, as the sample size increases, the gap disappears, leading us to believe with sufficient sample size, this difference in methods would be minimal.

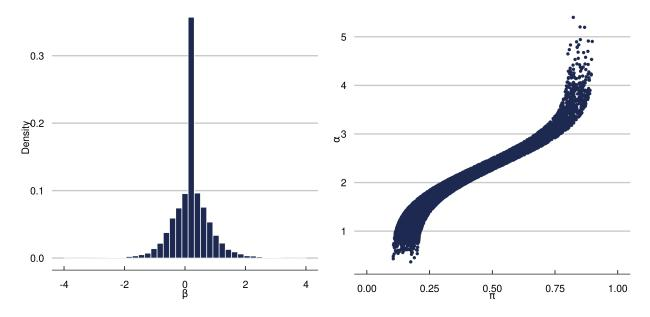


Figure 3: Left panel: Histogram of β . On the right is a plot of α vs π , indicative of strong targeted selection. For this particular realization of Equation 5, with n = 10,000, the mean of $\beta(X) = 0.20$, the mean of $\alpha(X) = 1.95$, and the range of $\pi(X) = (0.11,0.90)$, with mean of 0.37.

¹In the world of neural networks, this could entail changing dropout rates, implementing early stopping, or weight-decay, amongst other approaches. In general, an advantage of Neural Networks, particularly when using a well developed and maintained service like pyTorch is the ease in customizing one's model for one's needs.

Method	n	mean \hat{eta}	True ATE	True Mean α	Mean Runtime	Mean Correlation	Mean rMSE	mean (magnitude) Bias
Shared Network	250	0.47	0.20	1.95	45.38	0.74	0.50	0.26
BCF NNet	250	0.34	0.20	1.95	82.15	0.77	0.44	0.15
Separate Networks	250	0.40	0.20	1.95	33.00	0.69	0.57	0.19
OLS Approach	250	2.04	0.20	1.95	0.00	0.16	2.00	1.83
Shared Network	500	0.38	0.20	1.95	47.85	0.80	0.42	0.18
BCF NNet	500	0.28	0.20	1.95	87.10	0.83	0.37	0.10
Separate Networks	500	0.38	0.20	1.95	34.52	0.75	0.49	0.18
OLS Approach	500	2.04	0.20	1.95	0.00	0.21	2.00	1.84
Shared Network	1000	0.31	0.20	1.94	52.37	0.84	0.36	0.11
BCF NNet	1000	0.26	0.20	1.94	96.41	0.89	0.30	0.06
Separate Networks	1000	0.35	0.20	1.94	37.56	0.83	0.40	0.15
OLS Approach	1000	2.01	0.20	1.94	0.00	0.17	1.97	1.81

Table 1: Simulation results with small treatment to prognostic ratio. We run the DGP from Equation 5 with $\kappa=1.0$ across 100 independent trials (varying ε) for each size n. We generate X for each size n, but keep the X matrix the same for each of the 100 independent trials for each sample size (i.e. the X vary across the sample sizes, but are constant at each iteration per sample size). We train on the n size, but test on a size of 10,000, to ensure we are looking at population parameters. See Figure 4 if a visual presentation of this table is preferable.

Method	n	mean \hat{eta}	True ATE	True Mean α	Mean Runtime	Mean Correlation	Mean rMSE	mean (magnitude) Bias
Shared Network	250	4.89	5.00	1.94	46.00	0.60	0.62	0.14
BCF NNet	250	4.50	5.00	1.94	83.35	0.65	0.75	0.50
Separate Networks	250	4.85	5.00	1.94	33.49	0.49	0.87	0.19
OLS Approach	250	3.73	5.00	1.94	0.00	0.04	3.03	1.27
Shared Network	500	4.95	4.99	1.95	48.20	0.66	0.51	0.09
BCF NNet	500	4.66	4.99	1.95	88.01	0.74	0.54	0.34
Separate Networks	500	5.01	4.99	1.95	34.90	0.49	0.72	0.10
OLS Approach	500	3.76	4.99	1.95	0.00	0.05	3.01	1.24
Shared Network	1000	4.96	5.00	1.95	52.77	0.76	0.44	0.07
BCF NNet	1000	4.82	5.00	1.95	97.46	0.87	0.36	0.18
Separate Networks	1000	5.01	5.00	1.95	38.09	0.72	0.49	0.08
OLS Approach	1000	3.75	5.00	1.95	0.00	0.05	3.01	1.25

Table 2: Simulation results with large treatment to prognostic ratio. We run the DGP from Equation 5 with $\kappa=1.0$ across 100 independent trials (varying ε) for each size n. We generate X for each size n, but keep the X matrix the same for each of the 100 independent trials for each sample size (i.e. the X vary across the sample sizes, but are constant at each iteration per sample size). We train on the n size, but test on a size of 10,000, to ensure we are looking at population parameters. The benefits of the BCF NNet approach are lost, we hypothesize this is because any RIC introduced is offset by the large treatment, and since the treatment function compromises a good portion of the observed outcome, the extra parameters in the shared network should outperform the BCF NNet approach.

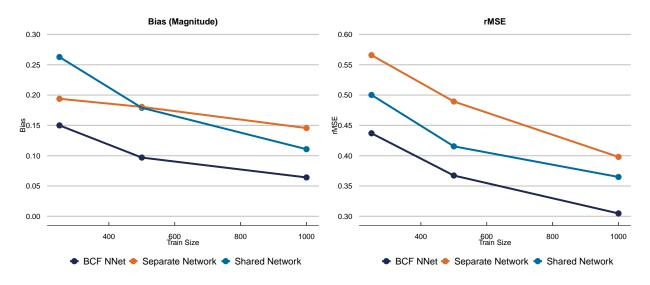


Figure 4: Left panel: Bias of dgp with different n. Right: RMSE. This is in the "small" β world.

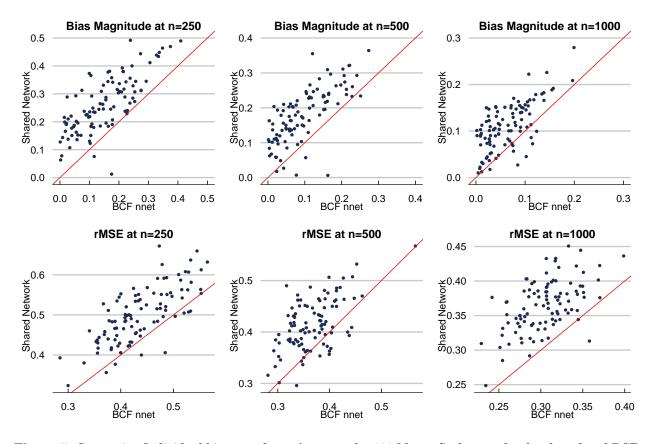


Figure 5: Comparing Individual biases and rmse's across the 100 Monte Carlo runs for the shared and BCF architectures.

5 Data Example

Onyper et al. [2012] is the data we look at as a demonstration of the methods. The dataset we are interested in has 253 observations with 1 treatment variable, 1 outcome variable, and 11 variables defining our feature space X. Specifically, the data is collected on participating undergraduate students at a liberal arts college in the northeastern United States. Our outcome is [Poor Sleep Quality], which is a range of integers from 1-18, with 1 being the worst sleep quality and 18 being the best (the metric of interest is called the "Pittsburgh Sleep Quality Index"), We standardize the data using the 'scale' command in R. The "treatment" we investigate is [Stress Level], where students respond with "high" or "normal". High stress level is considered the "treatment", and presumably should lead to lower sleep quality. However, this problem is a very clear causal inference problem, as illustrated in Figure 6. It is not unreasonable to expect there variables that could potentially lead to higher stress also lead to worse sleep quality, and in particular those described below. While this feature set likely does not fully meet the strong ignorability assumption, we still muster on with the example. The more worrying assumption violation is the SUTVA violation.

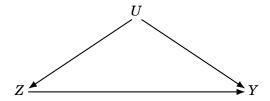


Figure 6: The classic graph.

- 1. Gender: Male/Female
- 2. Class Year: Fresh, Soph, Jr, Sr.
- 3. Early Class: Whether or not the student signed up for a class starting before 9AM
- 4. GPA: College GPA, scale 0-4
- 5. Classes Missed: Number of classes missed in semester
- 6. Anxiety Score: Measure of degree of anxiety
- 7. Depression Score: Measure of degree of anxiety
- 8. Happiness Score: Measure of degree of happiness
- 9. Number Drinks: Number of alcoholic drinks per week
- 10. All Nighter: Binary indicator for whether student had all-nighter that semester
- 11. Average Sleep: Average hours of sleep for all days

In our analysis, we change one hyper-parameter from our simulation study. For the propensity estimation, we only run 100 epochs instead of 250 epochs. In the simulation, we found that more epochs led to better predictive performance, but in the applied data problem, the propensity estimate clustered to estimates of 0 and 1 for the probability. As a benchmark, we compared our

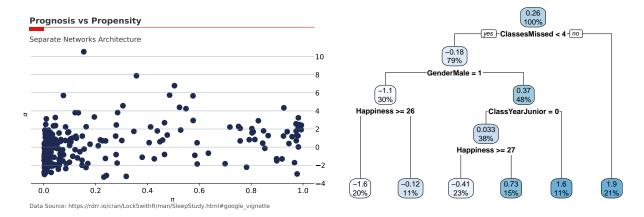


Figure 7: Left: A plot of $\alpha(X)$ vs $\pi(X)$, potentially indicative of targeted selection. Of course, in this example the selection is not targeted, but one could convince themselves people may be more stressed out if they start thinking about sleep problems. Right: A tree analysis, in the likes of Woody et al. [2020]. We fit a tree to treatment effects and analyze the effects of moderating variables.

fully connected 2-layer neural network estimate with a BART Chipman et al. [2010] estimate, and found that with 100 epochs the estimates were similar. Otherwise, all parameters stayed the same. Additionally, for this analysis we do not do a train/test split.

Method	CATE Estimate	Mean Prognostic
Shared Network	1.13	NA
Separate Networks	0.26	5.90
Separate Networks Bart Propensity	0.099	6.07
Naive NN Approach	-0.03	NA
BCF (R-implementation)	0.07	6.20

Table 3

6 Discussion

What is preferable about this proposed methodology to the state of the art tree methods, such as Wager and Athey [2018], Hahn et al. [2020], or Krantsevich et al. [2021]? We do not aim to answer that question, but rather instead provide some evidence that if a researcher is intent on using some deep learning architecture for their causal needs, then the methods developed in this document are the way to go. For one, we show in a plausible simulation study the benefits of our methodology. From a sheer performance point of view, our method provides an advantage over other competitive deep learning causal tools. Additionally, the parameterization of Hahn et al. [2020] provides multiple advantages. Because we split the prognosis and treatment networks, we can regularize the networks differently, we could use different hyperparameters for each, we can include different controls for each. This flexibility could likely be of importance to practitioners with expert knowledge. Additionally, because the approach is built off neural networks, it lends itself to other applications, such as incorporating image data into the control set (or even as a treatment). Building the network off pytorch also allows for easier scalability, adjustment, and online support.

Acknowledgements

We thank ASU Research Computing facilities for providing computing resources.

References

- Ran Chen and Hanzhong Liu. Heterogeneous treatment effect estimation through deep learning. *arXiv preprint arXiv:1810.11010*, 2018. 1
- Hugh A Chipman, Edward I George, Robert E McCulloch, et al. Bart: Bayesian additive regression trees. *The Annals of Applied Statistics*, 4(1):266–298, 2010. 6, 8, 14
- George Cybenko. Approximation by superpositions of a sigmoidal function. *Mathematics of control, signals and systems*, 2(4):303–314, 1989. 2
- Max H Farrell, Tengyuan Liang, and Sanjog Misra. Deep learning for individual heterogeneity. *arXiv* preprint arXiv:2010.14694, 2020. 1, 2, 5, 6, 7, 8, 10
- P Richard Hahn, Jared S Murray, and Carlos M Carvalho. Bayesian regression tree models for causal inference: Regularization, confounding, and heterogeneous effects (with discussion). *Bayesian Analysis*, 15(3):965–1056, 2020. 1, 2, 5, 6, 7, 8, 10, 14
- Miguel A Hernán and James M Robins. *Causal Inference: What If.* Boca Raton: Chapman & Hall, CRC, 2020. 2, 3, 4
- Jennifer L Hill. Bayesian nonparametric modeling for causal inference. *Journal of Computational and Graphical Statistics*, 20(1):217–240, 2011. 1, 5
- Nikolay Krantsevich, Jingyu He, and P Richard Hahn. Stochastic tree ensembles for estimating heterogeneous effects. *Arxiv Preprint*, 2021. URL https://arxiv.org/abs/2209.06998. 1, 14
- Serge V Onyper, Pamela V Thacher, Jack W Gilbert, and Samuel G Gradess. Class start times, sleep, and academic performance in college: a path analysis. *Chronobiology International*, 29(3):318–335, 2012. 13
- U. Shalit, F.D. Johansson, and D. Sontag. Estimating individual treatment effect: Generalization bounds and algorithms. *International Conference on Machine Learning*, 2017. 1
- Claudia Shi, David Blei, and Victor Veitch. Adapting neural networks for the estimation of treatment effects. *Advances in neural information processing systems*, 32, 2019. 1
- Stefan Wager and Susan Athey. Estimation and inference of heterogeneous treatment effects using random forests. *Journal of the American Statistical Association*, 113(523):1228–1242, 2018. 1, 5, 14
- C. Woody, S. Carvalho, P.R. Hahn, and J. Murray. Estimating heterogeneous effects of continuous exposures using bayesian tree ensembles: revisiting the impact of abortion rates on crime. Arxiv Preprint, 2020. 14